

Available online at [www.sciencedirect.com](http://www.sciencedirect.com)**ScienceDirect**

Procedia Engineering 127 (2015) 1189 – 1196

**Procedia  
Engineering**[www.elsevier.com/locate/procedia](http://www.elsevier.com/locate/procedia)

International Conference on Computational Heat and Mass Transfer-2015

## Flow Transients in Supercritical CO<sub>2</sub> Natural Circulation Loop

Archana V.<sup>a,\*</sup>, A. M. Vaidya<sup>b</sup>, P. K. Vijayan<sup>b</sup><sup>a</sup>Homi Bhabha National Institute, Mumbai – 400 094, India<sup>b</sup>Bhabha Atomic Research Centre, Mumbai – 400 085, India

### Abstract

A one-dimensional transient code is developed for studying the flow transient in the supercritical CO<sub>2</sub> natural circulation loop. The transient code is validated with the experimental result. Various flow transients such as flow initiation, power step up and power step back have been studied. The effect of operational parameters and geometrical parameters on flow initiation transient also has been studied. In all cases steady state has been reached and instability is not observed in vertical heater vertical cooler configuration of supercritical CO<sub>2</sub> natural circulation loop.

© 2015 The Authors. Published by Elsevier Ltd. This is an open access article under the CC BY-NC-ND license (<http://creativecommons.org/licenses/by-nc-nd/4.0/>).

Peer-review under responsibility of the organizing committee of ICCHMT – 2015

**Keywords:** Supercritical CO<sub>2</sub>; Natural circulation loop; flow initiation; power step up; power step back; Vertical heater vertical cooler

### 1. Introduction

In natural circulation loop, heat is transferred passively from heat source to heat sink without the use of any mechanical pumps. Natural circulation loop consists of a heat source at the lower elevation, sink at higher elevation and piping connecting source and sink. Heat transport by natural circulation of coolant is inherently safer due to its passive nature. In rectangular closed natural circulation loop, four configurations are possible by varying the heater and cooler positions namely, Horizontal Heater Horizontal Cooler (HHHC), Horizontal Heater Vertical Cooler (HHVC), Vertical Heater Horizontal Cooler (VHHC) and Vertical Heater Vertical cooler (VHVC).

Supercritical water reactor (SCWR) is one of the six nuclear reactors, selected by Gen IV International Forum (GIF) for further development. Instead of supercritical water, some reactor designs consider supercritical CO<sub>2</sub> as coolant [1]. Experiments involving supercritical water are expensive since they involve design and development of very high pressure and high temperature facilities. The variation of density, specific heat, viscosity and thermal

\*Corresponding author. Tel.: +91 2225591541; fax: +91 2225505151

E-mail address: [archanav@barc.gov.in](mailto:archanav@barc.gov.in)

conductivity of CO<sub>2</sub> with temperature at supercritical pressures is qualitatively similar to that of water. Hence, CO<sub>2</sub> is considered a good substitute for water for heat transfer studies.

**Nomenclature**

$D$	Diameter	$V$	Velocity (m/s)
$f_D$	Friction factor	$U$	Overall heat transfer coefficient (W/m <sup>2</sup> K)
$C_p$	Specific heat of fluid at constant pressure (J/kg K)	<i>Greek symbols</i>	
$g$	Gravitational acceleration (m/s <sup>2</sup> )	$\theta$	Angle with horizontal axis
$k_L$	Elbow loss coefficient	$\lambda$	Thermal conductivity (W/m K)
$P$	Pressure (Pa)	$\rho$	Density (kg/m <sup>3</sup> )
$q$	Heat flux (W/ m <sup>2</sup> )	<i>Dimensionless parameter</i>	
$r$	Radius	Re	Reynolds number
$T$	Temperature (K)		
$T_\infty$	Secondary side temperature (K)		

A supercritical pressure natural circulation loop (SPNCL) uses fluid above its critical pressure. A fluid heated to above the critical temperature and compressed to above the critical pressure is known as a supercritical fluid. In supercritical fluid, the phase change occurs from liquid like fluid to gas like fluid without forming any discontinuities in the fluid properties. In this paper various flow transients in vertical heater vertical cooler configuration of supercritical CO<sub>2</sub> natural circulation have been studied. The effect of various geometrical and operational parameters on flow initiation transient also has been studied.

**2. Experimental Setup**

The experimental set up of supercritical CO<sub>2</sub> natural circulation loop is shown in Figure 1.

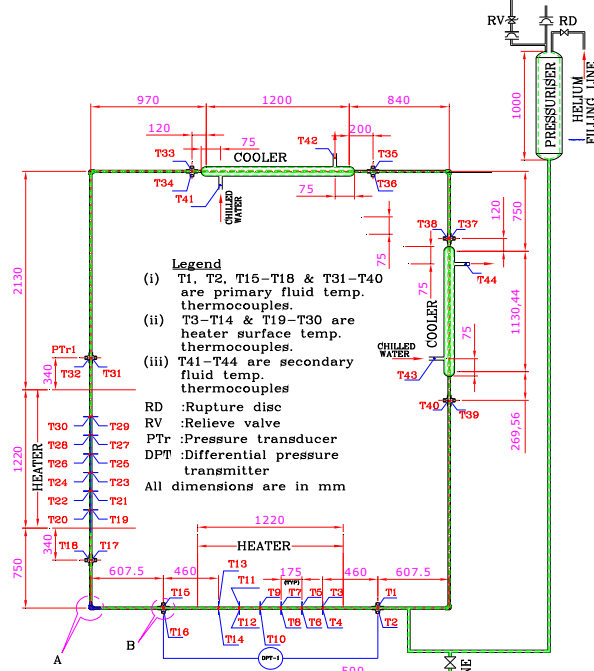


Figure 1 Schematic of SPNCL

Design details of this loop are published earlier [2] and only relevant details are given here. It is a uniform diameter rectangular loop with 13.88 mm inside diameter and outside diameter of 21.34 mm. The loop has two heater sections and two cooler sections. The loop can be operated in any one of the four orientations (HHHC, HHVC, VHHC or VHVC) by switching on one heater and one cooler. The cooler was tube-in-tube type heat exchanger with chilled water as secondary coolant flowing in the annulus. The CO<sub>2</sub> in the loop is pressurized to desired value by filling the cover gas (helium) above the carbon dioxide in the loop at appropriate pressure. The operating pressure is measured with the help of two pressure transducers. The fluid temperature is measured at heater inlet, heater outlet, cooler inlet and cooler outlet positions.

### 3. Numerical Model

One dimensional governing equations are derived by considering conservation of mass, momentum and energy over a small control volume. In one-dimensional analysis, the only spatial co-ordinate 's' runs around the loop. Variable property formulation is derived.

Transient 1D continuity, momentum and energy equations are given below

$$\frac{\partial}{\partial t}(\rho V) + \frac{d}{ds}(\rho V) = 0 \quad (1)$$

$$\frac{\partial}{\partial t}(\rho V) + \underbrace{\frac{\partial}{\partial s}(\rho V V)}_{\text{Convection}} = \underbrace{-\frac{\partial P}{\partial s}}_{\text{pressure gradient}} + \underbrace{\rho g \cos \theta}_{\text{component of fluid element weight in "s" direction}} - \underbrace{\left(\frac{f_D}{D} + K_L\right) \frac{\rho V^2}{2}}_{\text{friction at wall and elbow}} \quad (2)$$

$$\frac{\partial}{\partial t}(\rho C_p T) + \frac{\partial}{\partial s}(\rho V C_p T) = \frac{\partial}{\partial s} \left( \lambda \frac{\partial T}{\partial s} \right) + \underbrace{\frac{2q}{r}}_{\text{heat gain at source}} - \underbrace{\frac{2U}{r}(T - T_\infty)}_{\text{heat lost in sink}} + T \left[ \frac{\partial}{\partial s}(\rho V C_p) + \frac{\partial}{\partial t}(\rho C_p) \right] \quad (3)$$

The last term in equation (3) on RHS appears only in variable property formulation and is actually a part of convection term, hence it is modelled using upwind differencing. The third term in equation (3) appears only in heater section while fourth term is non-zero only in cooler section. Empirical correlations are used for heat transfer coefficient and friction factor. The secondary side flow is in turbulent region. Hence Dittus-Boelter equation is used for calculating the outside heat transfer coefficient ( $h_o$ ). Sharma et. al. [3] analyzed the predictability of different correlations for supercritical heat transfer coefficient and concluded that Bringer-Smith correlation gives better results. In view of this, the inside heat transfer coefficient ( $h_i$ ) is calculated using Bringer-Smith correlation [4]. Friction factor required in momentum equation is calculated using the following expression.

$$f_D = \text{MAX} \left( \frac{64}{\text{Re}}, \frac{0.316}{\text{Re}^{0.25}} \right) \quad (4)$$

where first component stands for laminar flow and 2<sup>nd</sup> stands for turbulent flow. This approach ensures transition from laminar to turbulent flow avoiding discontinuity in friction factor value and thereby avoiding numerical oscillation.

The governing equations are discretized using finite volume method [5]. The transient term is discretized using first order implicit method. The convection terms in the momentum and energy equations are discretized using first order upwind scheme. The diffusion term in energy equation is discretized using central difference method after integration over a control volume. Cyclic TDMA [6] is used for the solution of set of algebraic equations. The momentum, energy and pressure correction equations are coupled using SIMPLE algorithm. The convergence is ensured in each case by reducing the residuals of mass, momentum and energy equations to around 10<sup>-5</sup> at each time step.

### 4. Mesh and time independence study

Mesh independency was studied with different axial grid spacings such as 0.05 m, 0.02 m, 0.01 m and 0.005 m by keeping time step as 0.01s. The operating conditions are kept constant in each case. The heater power applied is 500 W, operating pressure is 85 bar, secondary side coolant inlet temperature is 280 K and the secondary side coolant flow rate is 40 lpm. The heater outlet mass flow rate using different axial grids is shown in Figure 2. The figure shows that mass flow rate profile computed using grid spacing of 0.01m and 0.005 m coincide with each other and only small deviation is there for other grid spacing. The cross sectional area used to calculate the mass flow rate is  $A = \pi \frac{D_i^2}{4}$ , where  $D_i$  is inside diameter of the pipe. Hence grid spacing taken for the further simulation is 0.01m.

Time independency was studied with different time step such as 0.02 s, 0.01 s and 0.005 s by keeping grid spacing as 0.01m. The heater outlet mass flow rate using different time step is shown in Figure 3. There is not much variation in heater outlet mass flow rate as the time step increases. But the increase in time step needs more SIMPLE iterations per time step, it takes more computational time with higher time step value. In order to optimize the computational time, a time step of 0.01s is fixed for further simulation.

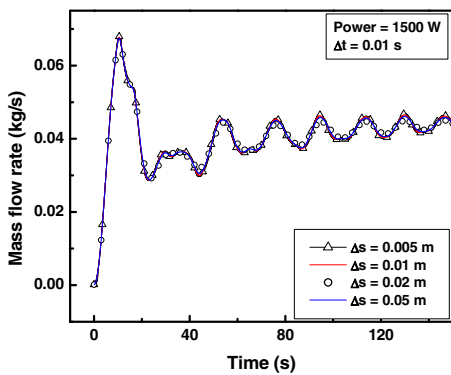


Figure 2 Mesh independence study

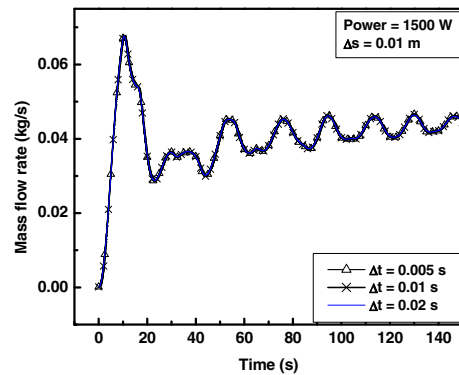


Figure 3 Time independence study

### 5. Validation

The code result is compared with the experimental result for VHHC case reported by Vijayan et al [7]. The experiment conditions are coolant flow rate is 5 lpm and inlet temperature of the coolant is 28°C and heater power of 232W at atmospheric pressure. The working fluid is water at atmospheric pressure. Time variation of pressure drop along the bottom horizontal pipe is computed for this power using transient code, which is shown in Figure 4. The figure shows that the result is qualitatively matching with the experimental results.

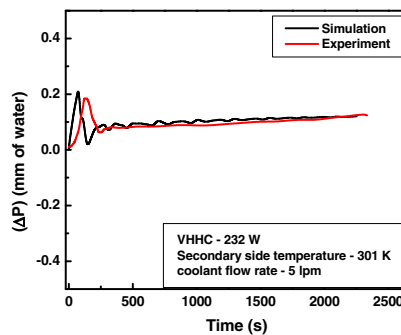


Figure 4 Validation of 1D code with experimental result

## 6. Results and Discussion

Various flow transients such as flow initiation, power step up and power step back have been studied. The effect of various parameters such as operational and geometrical parameter on the flow initiation transient studies also has been studied.

### 6.1. Flow initiation transient

In order to study the flow initiation transient in the natural circulation loop, the fluid is kept stagnant. A uniform initial temperature is specified which is same as that of secondary side temperature. A heater power is given to initiate the flow from the stagnant condition. The coolant flow rate is kept 40 lpm and coolant inlet temperature is kept 7<sup>o</sup> C at the cooler. The results plotted here are at a pressure of 85 bar. In VHVC, the left leg above heater is referred as the hot leg and the right leg below cooler is referred as the cold leg. The flow depends upon the pressure difference between these two legs. The heater is placed at the left vertical leg, this ensures the clockwise flow along the loop in the vertical heater vertical cooler configuration. The transient variations of heater outlet mass flow rate and temperature rise across heater for heater power of 500 W are shown in Figure 5. The transient variation of heater inlet, heater outlet, cooler inlet and cooler outlet temperature are plotted and is shown in Figure 6 for heater power of 500 W. The alternate play of friction force and buoyancy force causes the oscillations in the mass flow rate. Ultimately a steady state reaches at which the buoyancy force balances the frictional force.

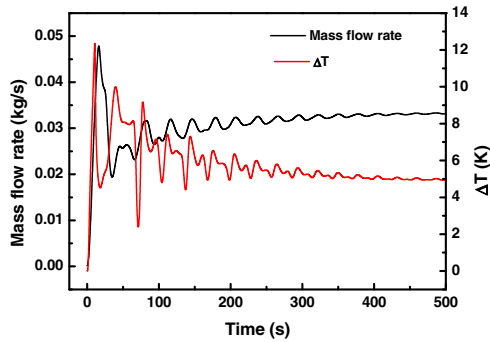


Figure 5 Transient variation of mass flow rate and temperature rise in heater at heater power of 500 W

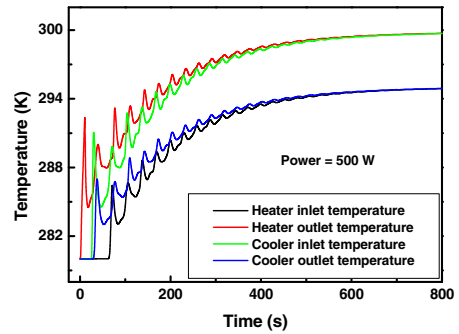


Figure 6 Transient variation of heater inlet and outlet, cooler inlet and outlet temperature at heater power of 500 W

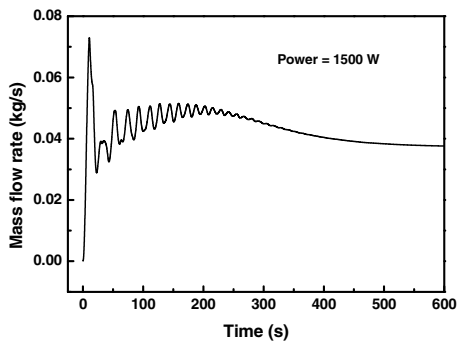


Figure 7 Transient variation of mass flow rate and temperature rise in heater at heater power of 1500 W

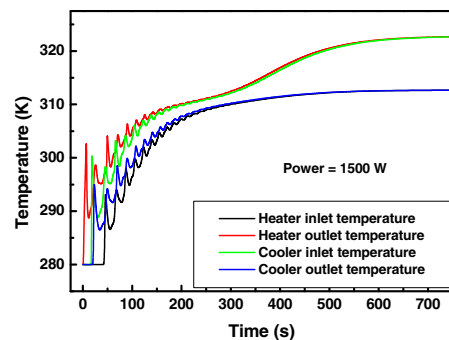


Figure 8 Transient variation of heater inlet and outlet, cooler inlet and outlet temperature at heater power of 1500 W

The transient variation of heater outlet mass flow rate for heater power of 1500 W is shown in Figure 7. The transient variation of heater inlet, heater outlet, cooler inlet and cooler outlet temperature are plotted and is shown in Figure 8 for heater power of 1500 W. The pseudo-critical temperature of CO<sub>2</sub> at pressure of 85 bar is 310.5 K. The heater outlet temperature for heater power of 500 W is below pseudo-critical point, so the transient is same as that of

subcritical flow. But the heater outlet temperature for heater power of 1500 W is above pseudo-critical point. The fluid initial temperature is below pseudo-critical point. As increasing the temperature, the density decreases rapidly for supercritical fluid. As the fluid passes through the pseudo-critical point, the fluid density decreases and hence frictional force increases which induce a reduction in mass flow rate and increase the heater outlet temperature.

6.2. Effect of operational parameters on flow initiation transient

Effect of operating parameter such as initial temperature, initial fluid velocity, coolant flow rate and operating pressure on flow initiation transient for heater power of 1500 W has been discussed in this section.

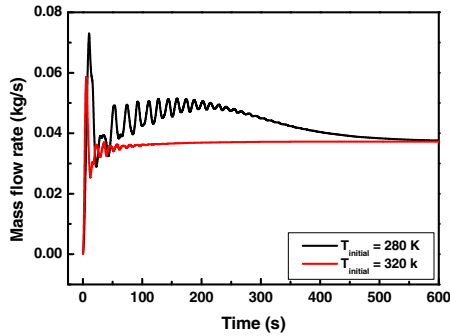


Figure 9 Effect of initial temperature on flow initiation transient

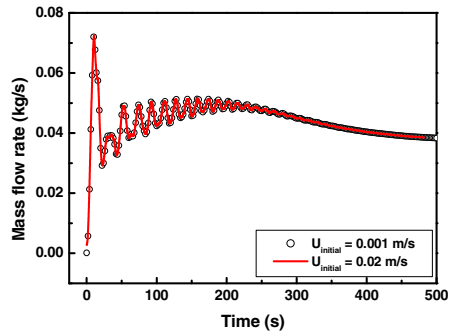


Figure 10 Effect of initial velocity on flow initiation transient

In order to study the effect of operational parameter, only one parameter is changed and others are kept constant. The flow initiation transients for different initial temperature such as 280 K and 320 K are shown in Figure 9. One initial temperature is below pseudo-critical point and other initial temperature is above pseudo-critical point. As the fluid goes through the pseudo-critical point the mass flow rate increases at around time of 150 second because of high density difference at that point. When the temperature reaches above the pseudo-critical point the density decreases drastically and the density difference also decreases, which makes the mass flow rate in loop to decrease beyond flow time of 200 second. When the temperature is above pseudo-critical point, the rise in mass flow rate is not observed around 150 second, since the density difference is less in that case. The flow initiation transients for different initial velocity such as 0.001 m/s and 0.02 m/s are shown in Figure 10. From the figure it can be concluded that the transient is not affected by the initial fluid velocity, since the steady state velocity is higher than the initial fluid velocity. The steady state value is not affected by the initial temperature and initial velocity.

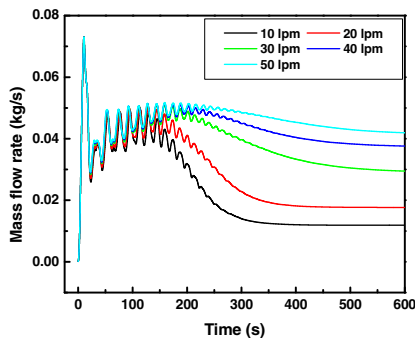


Figure 11 Effect of secondary side coolant flow rate on flow initiation transient

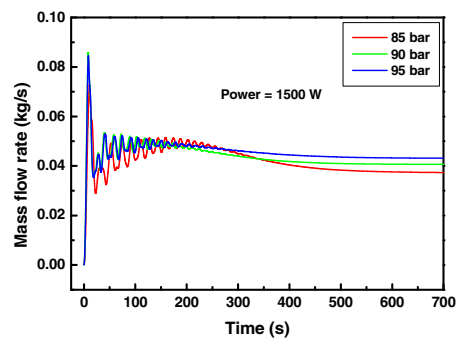


Figure 12 Effect of operating pressure on flow initiation transient

The effect of secondary side flow rate on flow initiation transient are studied by keeping different coolant volumetric flow rate such as 10, 20, 30, 40 and 50 lpm. The flow initiation transient for different coolant flow rate is shown in Figure 11. As increasing the coolant flow rate the steady state mass flow rate increases. This is because the average temperature in the loop decreases. The effect of operating pressure on flow initiation transient is studied by

changing the pressure such as 85, 90 and 95 bar. The flow initiation transient for different coolant flow rate is shown in Figure 12. The steady state mass flow rate is different in each case, this is because the density difference (driving force) is not same. The density difference is more for pressure of 95 bar and hence the mass flow rate is more compared to 85 bar.

### 6.3. Effect of geometrical parameters on flow initiation transient

The effects of geometrical parameters such as loop diameter and centreline elevation difference between heater and cooler on flow initiation transient for heater power of 1500 W are discussed in this section. The operational parameters are same as that mentioned in the previous section. The flow initiation transient for different loop diameter is show in Figure 13. The oscillation is more for loop diameter of 20 mm, since the loop friction is less. And oscillation is least for loop diameter of 6 mm since the loop friction is more. The steady state mass flow rate is different for each case, because of the friction. The higher friction causes the mass flow rate to decrease and the temperature in loop to increase.

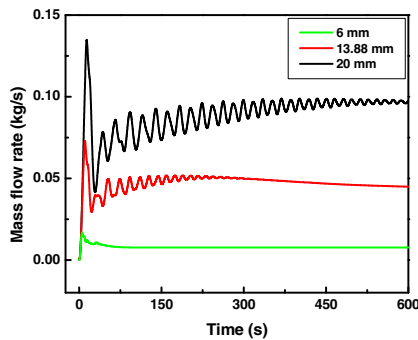


Figure 13 Effect of diameter on flow initiation transient

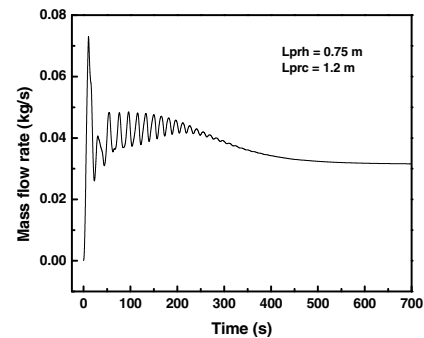


Figure 14 Flow initiation transient for Lprh=0.75m; Lprc=1.2m

The effect of centreline elevation difference between heater and cooler ( $\Delta z$ ) is studied by changing the length of pre-heater and pre-cooler length. Four case has been taken, first case is Lprh=0.75m; Lprc=0.75m;  $\Delta z=1.45$ m, the second case is Lprh=0.75m; Lprc=1.2m;  $\Delta z=0.975$ m, third case is Lprh=1.2m; Lprc=0.75m;  $\Delta z=0.975$ m and the fourth case is Lprh=1.2m; Lprc=1.2m;  $\Delta z=0.525$ m. The flow initiation transients for these cases are shown in Figure 7, Figure 14, Figure 15 and Figure 16 respectively.

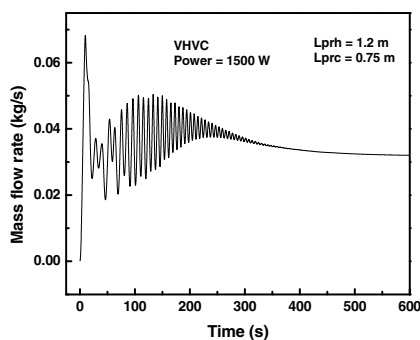


Figure 15 Flow initiation transient Lprh=1.2m; Lprc=0.75m

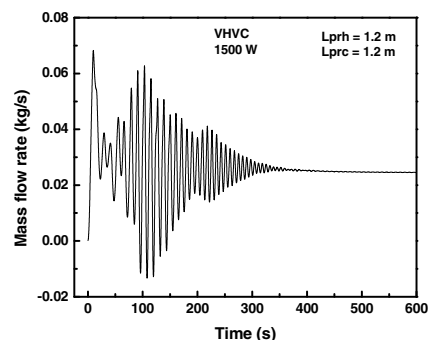


Figure 16 Flow initiation transient for Lprh=1.2m; Lprc=1.2m

The mass flow rate is higher in the first case, since the centreline elevation difference is higher in that case. As increase in the pre-cooler length does not have any effect in the transient. But increase in the pre-heater length shows more oscillations in the mass flow rate. In the fourth case the oscillation is more and even the flow reverses. But in all cases the flow is stabilized and no instability has observed for the VHVC configuration of SPNCL

#### 6.4. Power step up and step back transient

The power step up and step back transients are shown in Figure 17 and Figure 18.

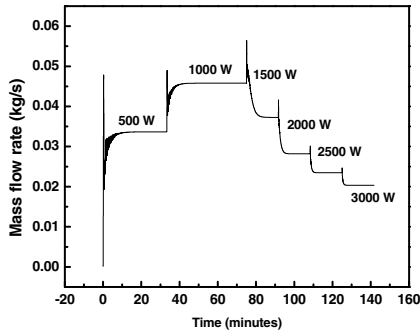


Figure 17 Transient variation of mass flow rate during power step up transient

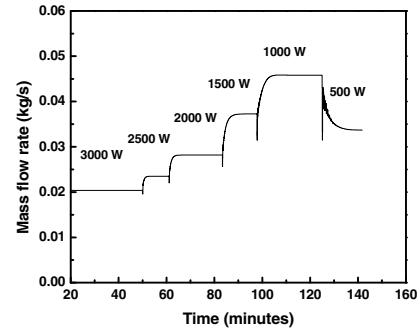


Figure 18 Transient variation of mass flow rate during power step back transient

The power step up study has been done by raising the heater power from 500 to 3000 W with a step of 500 W. The mass flow rate is plotted during the power step transient in Figure 17. As increase in the power, the steady state mass flow rate increases. But beyond the power of 1000 W, the mass flow rate decreases. This is because the density difference is maximum at pseudo-critical point. Beyond pseudo-critical point, the density difference decreases, which is the cause for mass flow rate to decrease. The power step back study has been done by decreasing the heater power from 3000 to 500 W with a step of 500 W. The mass flow rate is plotted during the power step transient in Figure 18. In both power step up and step back transient same steady state is achieved at corresponding power that means hysteresis is observed.

#### 7. Conclusion

A one-dimensional transient code is developed for studying the flow transient in the supercritical CO<sub>2</sub> natural circulation loop. The transient code is validated with the experimental result. Various flow transients such as flow initiation, power step up and power step back have been studied. The effect of operational parameters and geometrical parameters on flow initiation transient also has been studied. In all cases steady state has been reached and instability is not observed in vertical heater vertical cooler configuration of supercritical CO<sub>2</sub> natural circulation loop.

#### References

- [1]. Tom S.K.S., Hauptmann E.G., 1979, The feasibility of cooling heavy water reactors with supercritical fluids, Nuclear Engineering and Design 53 187–196
- [2]. Sharma M., D. S. Pilkhwal, S. S. Jana and P. K. Vijayan 2013a, A Test Facility for Heat Transfer Pressure Drop and Stability Studies under Supercritical Conditions, BARC/2013/E/002
- [3]. Sharma, M., Vijayan, P.K., Pilkhwal, D.S., Asako, Y., 2013b. Steady state and stability characteristics of natural circulation loops operating with carbon dioxide at supercritical pressures for open and closed loop boundary conditions. Nucl. Eng.Des. 265, 737–754.
- [4]. Piro I L., Hussam F. Khartabil, Romney B. Duffey 2004, Heat transfer to supercritical fluids flowing in channels—empirical correlations (survey), Nuclear Engineering and Design 230 69–91
- [5]. Patankar S. V. 1980, Numerical heat transfer and fluid flow, Hemisphere Publishing Corporation
- [6]. Patankar S. V., C. H. Liu, E. M. Sparrow 1977, Fully developed flow and heat transfer in ducts having stream wise-periodic variations of cross-sectional area, Transactions of ASME, 99 180-186
- [7]. Vijayan P. K., Bhojwani V. K., Bade M. H., Sharma M., Nayak A. K., Saha D. And Sinha R. K. 2001, Investigation on the effect of heater and cooler orientation on the steady state, transient and stability behaviour of single-phase natural circulation in a rectangular loop. BARC/2001/E/034